ATPase reaction cycle of P4-ATPases affects their transport from the endoplasmic reticulum

Takuya Tone[1], Kazuhisa Nakayama[1], Hiroyuki Takatsu[1], and Hye-Won Shin[1*]
[1] Department of Physiological Chemistry, Graduate School of Pharmaceutical Sciences, Kyoto University, Sakyo-ku, Kyoto 606-8501, Japan

[*] Correspondence should be addressed to H.-W.S. (e-mail: shin@pharm.kyoto-u.ac.jp)

ABSTRACT

P4-ATPases belonging to the P-type ATPase superfamily mediate active transport of phospholipids across cellular membranes. Most P4-ATPases form heteromeric complexes with CDC50 proteins, which are required for transport of P4-ATPases, except ATP9A and ATP9B proteins, from the endoplasmic reticulum (ER) to their final destinations. P-type ATPases form auto-phosphorylated intermediates during the ATPase reaction cycle. However, the association of the catalytic cycle of P4-ATPases with their transport from the ER and their cellular localization has not been studied. In this study, we showed that transport of ATP9 and ATP11 proteins, and ATP10A from the ER depends on the ATPase catalytic cycle, suggesting that conformational changes in P4-ATPases during the catalytic cycle are crucial for their transport from the ER.

Keywords: membrane, lipid bilayer, flippase, P4-ATPase, E1-E2 ATPase

INTRODUCTION

P-type ATPases constitute a large superfamily that transport ions and lipids across cellular membranes using ATP as an energy source. The transport process by P-type ATPases takes place according to the Post–Albers cycle [1-3], which involves four major conformations; E1, E1P, E2P, and E2. These conformations involve large movements of three cytoplasmic domains; N (nucleotide binding), P (phosphorylation), and A (actuator) [1,4-7]. The main characteristic of all P-type ATPases is formation of a phosphoenzyme intermediate (EP). An aspartate residue in the highly conserved DKTGT sequence motif in the P domain is transiently phosphorylated during the ATPase catalytic cycle. Moreover, a glutamate residue in the highly conserved TGES/DGET sequence motif in the A domain is critical for the dephosphorylation of the phosphoaspartate residue. The phosphorylation and dephosphorylation are tightly coupled to binding, transport, and release of substrates [4-9].

P4-ATPases belonging to the P-type ATPase superfamily flip membrane lipids from the exoplasmic to the cytoplasmic leaflet of biological membranes to regulate the transbilayer lipid asymmetry [7,10-12]. In humans, 14 members of the P4-ATPase family are expressed in various cell types and tissues, and translocate specific substrates, not only glycerophospholipids, such as phosphatidylserine, phosphatidylethanolamine, phosphatidylcholine, but also a glycosphingolipid, glucosylceramide [11,13-18]. Mutations in some of these P4-ATPases, such as ATP8A2, ATP8B1, and ATP11C, are linked to hereditary diseases [19-23]. The amino acid sequence similarity of P-type ATPases indicates that the overall structure and domain organization of P4-ATPases resemble those of other P-type ATPases, such as Ca^{2+}-ATPase (SERCA) and Na^{+}/K^{+}-ATPase [7,24,25]. While submitting the present manuscript, the cryo-EM structures of Drs2p/Cdc50p and ATP8A1/CDC50A have been reported and the ATPase reaction cycle, which is similar to other P-type ATPases, has been elucidated [26,27], although little is known about the actual mechanism of lipid translocation.

We and others previously showed that interaction of most P4-ATPases (P4A clade, based on a revised phylogenetic analysis of P4-ATPases), except for ATP9A and ATP9B (P4B clade), with CDC50 proteins is crucial for their cellular localization [13,28-31]. Mutation of the aspartate residue within the DKTGT sequence motif does not allow some P4-ATPases to exit the ER [11,29] and probably inhibits their interaction with CDC50 proteins [32,33]. However, the role of the catalytic cycle of P4-ATPases, including ATP9A and ATP9B, in their transport from the ER and their cellular localization has not been examined.

In this study, we found that ATP9A and ATP9B, which are able to exit the ER in a

CDC50A-independent manner, remain trapped in the ER by the mutation of the aspartate residue. On the other hand, their mutants of the glutamate residue in the DGET motif (dephosphorylation-deficient mutation), were able to exit the ER. These findings suggest that, in addition to their lipid-transporting activities, the transport of P4-ATPases from the ER to cellular compartments is associated with their ATPase reaction cycle.

MATERIALS and METHODS

Plasmids

Expression vectors for C-terminally HA-tagged human P4-ATPases (ATP9A, ATP9B, ATP10A, ATP11A, ATP11B, and ATP11C) and N-terminally FLAG-tagged human CDC50A and CDC50B were constructed as described previously [11,16,34]. Point mutations of P4-ATPases were introduced into the cDNAs using the QuikChange II XL Site-Directed Mutagenesis Kit (Agilent Technologies) or a PCR-based strategy using mutagenic primers, and the seamless ligation cloning extract (SLiCE) method [35]. Oligonucleotides for the mutagenesis are shown in Supplementary Table. Each mutation was confirmed by sequencing analysis. A cDNA for vesicle-associated membrane protein–associated protein A (VAPA) was cloned from a human brain cDNA library using polymerase chain reaction and inserted into an enhanced green fluorescent protein plasmid (pEGFP) vector (Clontech Laboratories).

Antibodies and reagents

Anti–CDC50A antisera were raised in rabbits against a mixture of two peptides synthesized by MBL: (C)APGGTAKTRRPDNT and (C)NHKYRNSSNTADITI; amino acids 17–31 and 347–361, respectively. The antisera were affinity purified using the peptide immobilized on Sulfolink beads (Pierce Chemical). To examine the specificity of the affinity purified antibody, immunoblot analyses were performed using cell lysates from HeLa cells expressing CDC50A or CDC50B and immunoprecipitates with anti-DYKDDDDK antibody of each lysate (Supplementary Figure S1). The sources of other antibodies used in this study were as follows: monoclonal rat anti-HA (3F10) (Roche Applied Science); monoclonal mouse anti-EEA1, and anti-p230 (BD Biosciences); monoclonal mouse anti-DYKDDDDK (1E6) (Wako Chemicals) and anti-β-tubulin (KMX-1; EMD Millipore); monoclonal rabbit anti-ATP1A1 (EP1845Y; Abcam); Alexa Fluor 488–conjugated secondary antibodies (Molecular Probes); and Cy3-conjugated and horseradish peroxidase (HRP)-conjugated secondary antibodies

(Jackson ImmunoResearch Laboratories).

Cell culture and establishment of stable cell lines

HeLa cells were cultured in minimal essential medium (Nacalai Tesque) supplemented with 5% heat-inactivated fetal bovine serum (FBS) at 37 °C under a 5% CO_2 atmosphere. To transiently express P4-ATPases, HeLa cells were transfected with expression plasmids for P4-ATPases and/or CDC50A using FuGENE6 (Promega) and incubated for 48 h. For retroviral production, pMXs-neo-derived vectors for expression of HA-tagged P4-ATPases were co-transfected with pEF-gag-pol and pCMV-VSVG-Rsv-Rev into HEK293T cells, as described previously [11]. The resultant retroviruses were concentrated and then used to infect HeLa cells to establish stable cell lines.

Immunofluorescence analysis

HeLa cells were fixed with 3% paraformaldehyde in phosphate-buffered saline (PBS) at room temperature for 15 min and quenched with 50 mM NH_4Cl in PBS at room temperature for 15 min. Then, the cells were permeabilized with 0.1% TritonX-100 in PBS at room temperature for 5 min and blocked with 10% FBS in PBS at room temperature for 30 min. Finally, the cells were incubated sequentially with primary and secondary antibodies at room temperature for 1 h. Coverslips were placed onto Mowiol mounting medium, and the cells were observed under an Axiovert 200M microscope (Carl Zeiss).

Immunoprecipitation

HeLa cells were lysed in lysis buffer (20 mM 4-(2-hydroxyethyl)-1-piperazineethanesulfonic acid [HEPES]-KOH, pH 7.4; 150 mM NaCl; 1 mM ethylenediaminetetraacetic acid [EDTA]; 1% NP-40) containing a protease inhibitor cocktail (Nacalai Tesque) and kept on ice for 30 min. Then, the cell lysates were centrifuged at 16,100 × *g* at 4 °C for 30 min in a microcentrifuge. The supernatant was incubated with an anti–HA antibody at 4 °C for 15 min and mixed with protein G–coupled Dynabeads (Invitrogen) at 4 °C overnight. After washing, proteins were eluted from the beads using sodium dodecyl sulfate-polyacrylamide gel electrophoresis (SDS-PAGE) sample buffer, denatured at 37 °C for 2 h, separated by SDS-PAGE, and electroblotted onto an Immobilon-P transfer membrane (EMD Millipore). Next, the membrane was blocked using 5% bovine serum albumin in Tris-buffered saline with Tween 20 (TBS-T) and incubated sequentially with primary and HRP-conjugated

secondary antibodies. Finally, detection was carried out using a Chemi-Lumi One Super kit (Nacalai Tesque). Images were recorded on a LAS-3000 Bioimaging system (Fujifilm).

RESULTS AND DISCUSSION

Role of the ATPase reaction cycle in the cellular localization of ATP11 proteins

Figures 1A–C show the crystal structures of SERCA (E1P and E2P conformations), the cryo-EM structure of Drs2p, and the model structure of the ATP9A protein created using Phyre^2 software [36], respectively. The mechanism of ATP-dependent phosphorylation and dephosphorylation is conserved in all P-type ATPases [1,7,27,37]. In particular, the aspartate residue (D351, D560, and D391 in Figure 1A–D) within the highly conserved DKTGT sequence motif in the P-domain is phosphorylated, and the TGES/DGET motif in the A-domain (especially E183, E342, and E195 in Figure 1A–D) is critical for dephosphorylation during the ATPase reaction cycle [7,38-40]. The phosphorylated and ADP-bound form of the ATPase is denoted as E1P-ADP in Figure 1A (3BA6). In the A-domain of SERCA, E183, which is critical for dephosphorylation, is located away from the phosphorylated D351 in the E1P conformation. ADP release clears a binding site for the TGES loop of the A-domain and allow docking of the TGES loop on the P-domain near the phosphorylated aspartate residue. And thus, E183 is adjacent to the phosphorylated D351 in the E2P conformation (Figure 1A; 1WPG). Figure 1E shows a scheme of the P-type ATPase catalytic cycle. Mutation of the aspartate to asparagine in the DKTGT motif prevents phosphorylation and enzyme activity. Mutation of the glycine to leucine in the TGES/DGET motif allows phosphorylation that forms E1P, but inhibits the E1P–E2P transition, resulting in trapping of the enzyme in the E1P conformation. Mutation of the glutamate to glutamine in the TGES/DGET motif inhibits dephosphorylation of E2P to E2, resulting in trapping of the enzyme in the E2P conformation (Figure 1D) [6,39-41].

We previously showed that mutation of glutamate to glutamine (EQ mutation) in P4-ATPases does not affect their cellular localization but abrogates their flippase activities toward NBD-labeled lipids [11,14,16]. On the other hand, mutation of aspartate to asparagine (DN mutation) inhibits the exit of P4-ATPases from the ER and some DN mutants could not interact with CDC50 proteins [11,29,32,33]. In order to examine the relationship between the ATPase reaction cycle and cellular localization of P4-ATPases, we substituted the aspartate in the DKTGT motif, or glycine or glutamate residue in the DGET motif of human P4-ATPases (ATP11A, ATP11B, and ATP11C, PS/PE-flippases; ATP10A, PC-flippase [11,15,16]) with the asparagine, leucine, or glutamine residue, respectively (Figure 1D,E), and observed their cellular localization (Figure 2). The ATP11 proteins and ATP10A require the CDC50A protein for their transport from the ER and appropriate cellular localization [16,34]. We therefore

transiently co-expressed each mutant of ATP11A, ATP11B, ATP11C, or ATP10A, which is C-terminally tagged with HA, and N-terminally FLAG-tagged CDC50A, and investigated their localization with organelle markers by immunofluorescence analysis (Figure 2). ATP11A(WT), ATP11C(WT), and ATP10A(WT) localized to the plasma membrane and ATP11B(WT) to early/recycling endosomes but not to late endosomes (Figure 2A,C,E,F,I, a-a‴) [16,34]. In addition, the ATP11A(EQ), ATP11B(EQ), ATP11C(EQ) and, ATP10A(EQ) mutants localized to the plasma membrane and endosomes, similarly to WT enzymes (Figure 2A,C,E,F,I, d-d‴). In contrast, ATP11A(DN), ATP11B(DN), ATP11C(DN) and ATP10A(DN) mutants did not localize to the plasma membrane or endosomes (Figure 2A,C,F,I, b-b‴), but remained in the ER (Figure 2B,D,G,J, b-b‴), indicating that inhibition of E1–E1P transition inhibits the transport of enzymes from the ER. In addition, ATP11A(GL), ATP11C(GL) and, ATP10A(GL) mutants did not localize to the plasma membrane (Figure 2A,F,I, c-c‴) but remained in the ER (Figure 2B,G,J, c-c‴), indicating that suppression of the E1P–E2P transition inhibits the transport of the ATP11 proteins and ATP10A from the ER. On the other hand, a large proportion of the ATP11B(GL) mutant localized to early/recycling endosomes (Figure 2C, c-c‴), and its small proportion remained in the ER (Figure 2D, c-c‴). Counting the number of cells in which ATP11B or their mutants localized to endosomes, to both endosomes and the ER, and to the ER only (Figure 2H), we revealed that most of the ATP11B(DN) mutant remained in the ER, whereas ATP11B(WT) and ATP11B(EQ) mutant localized to endosomes (Figure 2H). Although a significant proportion of the ATP11B(GL) mutant remained in the ER, a large proportion also localized to endosomes. These observations indicate that efficient transport of the ATP11 proteins and ATP10A from the ER requires the E1P–E2P transition.

Interaction between P4-ATPases and endogenous CDC50A is altered during the ATPase reaction cycle

Since the ATP11 proteins and ATP10A are transported from the ER and localized to cellular compartments in a CDC50A-dependent manner [16,34], we investigated the interaction of the ATP11 and ATP10A mutants with CDC50A. To exclude overexpression artifacts, we established cells stably expressing HA-tagged ATP11 proteins, ATP10A, and their mutants and examined whether endogenous CDC50A was co-immunoprecipitated with the P4-ATPases (Figure 3). Mildly expressed ATP11 proteins and ATP10A in stable cells were transported from the ER normally to the plasma membrane or endosomes, even in the absence of exogenous expression of

CDC50A. In addition, we detected flippase activities of the enzymes in the plasma membrane in the absence of exogenous CDC50A expression, indicating that the endogenous level of CDC50A is sufficient for P4-ATPase transport in the stable cells [11,14,16]. In fact, in cells stably expressing ATP11A-HA or ATP11B-HA, both enzymes accumulate in the ER by depletion of endogenous CDC50A using short interfering RNAs [16,34]. To detect endogenous CDC50A, we raised a polyclonal anti-CDC50A antibody and confirmed that the antibody specifically detected CDC50A (Supplementary Figure 1).

The WT and EQ mutants of each ATP11 protein and ATP10A co-immunoprecipitated endogenous CDC50A (Figure 3A,C), indicating that the E2P conformation of ATP11 proteins and ATP10A interact with CDC50A. The CDC50A protein migrated as broad bands (Figure 2, asterisks) due to a high level of N-glycosylation [30,34,42]. However, we hardly detected the CDC50A protein co-immunoprecipitated with ATP11A(GL), ATP11C(GL) and, ATP10A(GL) mutants and with the DN mutants of all ATP11 and ATP10A. By contrast, the ATP11B(GL) mutant co-immunoprecipitated a significant amount of CDC50A. Because all ATP11(EQ) mutants and the ATP11B(GL) mutant were transported from the ER (Figure 2), these data indicate that the interaction of the ATP11 and ATP10A with CDC50A is correlated with their transport from the ER. These data also suggest that the ATP11–CDC50A interaction fluctuates during the ATPase reaction cycle of the P4-ATPases. These results are consistent with previous studies showing that the DN and GL mutants of yeast P4-ATPase Drs2p do not interact with Cdc50p [32]. Therefore, conformational changes in the ATP11 proteins and ATP10A during the ATPase reaction cycle influence their interaction with CDC50A. As shown in Figure 3B and D, the expression levels of the GL and DN mutants were lower than those of the WT protein and the EQ mutants, suggesting that, in the absence of the CDC50A interaction, the GL and DN mutants were degraded by a quality control mechanism in the ER. Given that coexpression of CDC50A increased the expression levels of ATP8A and ATP8B proteins compared with the expression levels of the P4-ATPases when transfected alone [30], CDC50A could stabilize P4-ATPases. We also cannot exclude a possibility that the two mutants are not properly folded or less stable than WT and subsequently can be degraded.

How is the CDC50A interaction with P4-ATPases regulated during the ATPase reaction cycle? Because CDC50A interacted with all ATP11(EQ) and ATP10A(EQ) mutants but did not interact with ATP11A(GL), ATP11C(GL), and ATP10A(GL), stable interaction of CDC50A requires the E2P conformation of the P4-ATPases. Drs2p phosphoenzyme intermediate (EP) was readily formed in the presence of Cdc50p and

seemed to be stabilized at the E2P stage [32]. Moreover, we detected a larger amount of the CDC50A protein co-immunoprecipitated with the ATP11A(EQ) mutant compared with ATP11A(WT) (Figure 3A and E). Therefore, the CDC50 protein might stabilize the E2P conformation of P4-ATPases, preventing dephosphorylation that is in a good agreement with the previous result of Cdc50p and Drs2p [32]. Notably, a significant proportion of the ATP11B(GL) mutant interacted with CDC50A and was transported from the ER. One possibility is that the ADP-released E1P conformation of ATP11B may resemble its E2P conformation, allowing interaction with CDC50A. Although the rate of the Ca_2E1P–E2P transition in the SERCA(GL) mutant is 10-100-fold slower than that of wild type [39], another possibility is that the rate of E1P–E2P transition in ATP11B(GL) mutant is faster than that in ATP11A(GL) and ATP11C(GL). Although the recent cryo-EM structure of ATP8A1/CDC50A shows that CDC50A seems to interact with ATP8A1 through the ATPase reaction cycle [27], the coimmunoprecipitation data (Figure 3A and C) suggests that the interaction of DN and GL mutants with CDC50A is unstable or its affinity is very low.

The ATPase activity of P4-ATPases can be stimulated by their substrates but not by other lipids [15,18,43-45], indicating that incorporation of substrates triggers dephosphorylation, thereby allowing the E2P–E2 transition. The flipped lipids are then released from P4-ATPases via an unknown mechanism, and P4-ATPases return to the ground-state E1 conformation.

ATP9A and ATP9B proteins did not interact with endogenous CDC50A proteins

We previously showed that, when transiently expressed, ATP9A localized to endosomes and the trans-Golgi network (TGN) and ATP9B to the TGN in a CDC50A-independent manner [34]. We further investigated whether the ATP9A and ATP9B proteins interact with endogenous CDC50A in cells stably expressing ATP9A, ATP9B, and their mutants (Figure 3E). Endogenous CDC50A was not co-immunoprecipitated with ATP9A or ATP9B proteins, or their mutants, confirming that the ATP9A or ATP9B protein do not interact with endogenous CDC50A (Figure 3E) as well as exogenous CDC50A [34]. As shown in Figure 3F, the expression levels of the GL and DN mutants of ATP9 proteins were lower than those of the WT and EQ mutant. The GL and DN mutants may be less stable than the WT and EQ mutant or may not be properly folded and subsequently can be degraded. It also has been shown that the ATP8A2(D416N) and ATP8B1(D454G, found in progressive familial intrahepatic cholestasis 1 patients) mutants were expressed at a lower level compared to WT [11,44] and the Drs2p(D560N) mutant was purified at very low levels even if the expression

levels of Drs2p(WT), Drs2p(EQ), and Drs2p(DN) were almost the same [46] supporting that the DN mutant is less stable than the WT and EQ mutant. Therefore, although the DN mutant has been used in many biochemical studies of P-type ATPases, the EQ mutant would be a better negative control for functional studies of P4-ATPases.

EP conformation of ATP9A and ATP9B is required for transport from the ER

Next, we examined cellular localization of ATP9A and ATP9B proteins and their DN, GL, and EQ mutants. When transiently expressed as C-terminally HA-tagged protein, ATP9A localized to the TGN and endosomes (Figure 4A and C, a-a‴), whereas ATP9B localized to the TGN (Figure 4D, a-a‴), even in the absence of exogenous CDC50A expression as shown previously [34]. The ATP9A(EQ) and ATP9B(EQ) mutants localized to endosomes and the TGN, similar to WT enzymes (Figure 4A,C,D, d-d‴), indicating that the ATP9 protein can be transported normally from the ER to cellular compartments in their E2P conformation. In contrast, ATP9A(DN) and ATP9B(DN) mutants did not localize to the TGN or endosomes (Figure 4A,C,D, b-b‴), but remained in the ER (Figure 4B,E, b-b‴), indicating that inhibition of the E1–E1P transition suppresses the transport of the enzymes from the ER. The ATP9A(GL) mutant also remained in the ER (Figure 4B, c-c‴), but did not localize to the TGN or endosomes (Figure 4A,C, c-c‴). On the other hand, a significant proportion of the ATP9B(GL) mutant localized to the TGN (Figure 4D, c-c‴), although a large proportion was observed in the ER (Figure 4E, c-c‴). Exogenous expression of CDC50A did not change the cellular localization of the ATP9(WT) proteins or their mutants (Supplementary Figure S2). We also confirmed that the cellular localizations of ATP9 and ATP11 proteins and their mutants in stably expressing cells (Supplementary Figure S3) were similar to those in transiently expressing cells (Figures 2 and 4). Counting the number of cells in which ATP9B or its mutants localized to the Golgi only, to the Golgi and the ER, and to the ER only (Figure 4F), most of the ATP9B(DN) mutant was revealed to remain in the ER, whereas ATP9B(WT) and ATP9B(EQ) mutants localized to the TGN (Figure 4H). Although a large proportion of the ATP9B(GL) mutant remained in the ER, a significant proportion localized to the TGN (Figure 4D-F). Therefore, suppression of the E1P–E2P transition substantially inhibits the ATP9A transport but partially inhibits the ATP9B transport from the ER. These observations suggest that at least the EP formation is required for the transport of ATP9A and ATP9B from the ER. In particular, the E2P conformation of ATP9A and ATP9B is required for their efficient transport from the ER. Notably, some proportion of the ATP9B(GL) mutant was transported from the ER. One possibility is that the rate of the E1P–E2P

transition in ATP9B(GL) mutant is rather faster than that in ATP9A(GL). Because ATP9A and ATP9B did not require CDC50A for the transport from the ER, their conformational changes during the ATPase reaction cycle could directly affect the transport from the ER.

Although it is unknown how ATP9A and ATP9B proteins can exit the ER without interaction with CDC50A, their cytoplasmic regions might play an important role in their transport and targeting to intracellular compartments. In fact, the N-terminal cytoplasmic region of ATP9B is critical for its localization to the TGN, and the C-terminal regions of ATP11C isoforms determine their differential cellular localization [34,47,48]. In addition, the N-terminal region of ATP13A2 (P5-ATPase) is required for its lysosomal targeting via interacting with phosphatidic acid and phosphatidylinositol-3,5-bisphosphate [49], and ATP7A and ATP7B (P1B-ATPases) likely harbor intracellular trafficking signals in their C-terminal region[50]. Moreover, the C-terminal regions of Drs2p and ATP8A2 seem to play an important role in their enzymatic activities [51-53]. Therefore, the ATPase reaction cycle accompanied by conformational changes in N- and/or C-terminal cytoplasmic regions of ATP9A and ATP9B is expected to play a key role in their transport from the ER and their cellular localization and possibly in their enzymatic activities.

Taken together, these findings suggest that newly synthesized P4-ATPases seem to progress through the reaction cycle at least once in the ER for quality control, which is consistent with the substrate-independent autophosphorylation of P4-ATPases [44], although it is unknown whether dephosphorylation can occur efficiently in the ER. In particular, the E2P conformation could be important for their transport from the ER, even in the absence of the CDC50 protein. CDC50A interacts with of ATP11A/B/C and ATP10A proteins in the E2P conformation during their transport from the ER and possibly stabilizes the conformation [32]. Because the EP formation is also required for transport of ATP9A and ATP9B from the ER, it remains to be elucidated how the E2P conformation of ATP9A and ATP9B can be stabilized by preventing dephosphorylation during their transport from the ER even without CDC50A. In one hand, a possibility of the presence of another interacting protein for ATP9 proteins instead of CDC50 cannot be excluded. A substrate is believed to bind the E2P conformation (Figure 1D) and to trigger dephosphorylation of E2P [15,42-44,54]. It is tempting to speculate that intrinsic ATPase activities of the ATP9 proteins are low in the lipid environment of the ER or that lipid substrates are not abundant in the ER membranes and thus the E2P conformation can be sustained during the exit from the ER. Our finding raises the big question of how conformational changes of ATP9 proteins regulate protein transport

from the ER and how those of ATP11 proteins and ATP10A regulate the interaction with CDC50A.

Acknowledgments

We thank Toshio Kitamura (The University of Tokyo) and Hiroyuki Miyoshi (RIKEN BioResource Center) for kindly providing plasmids for retroviral infection. We thank Hiroshi Suzuki (Asahikawa Medical University) for critical comments on the manuscript. We also thank Ms. Keiko Baba for a technical assist in the antibody production. This work was supported by JSPS KAKENHI Grant Numbers JP17H03655 (to H.-W.S.) and JP17K08270 (to H.T.); the Takeda Science Foundation (to H.-W.S.); the Japan Foundation for Applied Enzymology (to H.-W.S); and the Naito Foundation (to H.-W.S.).

Author contributions

H.-W.S. conceived and designed the experiments. T.T., and H.T. performed the experiments. T.T., H.T., and H.-W.S analyzed the data. H.-W.S wrote the manuscript. All authors discussed results and commented on the manuscript.

There are no conflicts of interest to declare.

References

1. Kuhlbrandt W: Biology, structure and mechanism of P-type ATPases. *Nat Rev Mol Cell Biol* 2004, 5:282-295.
2. Post RL, Hegyvary C, Kume S: Activation by Adenosine Triphosphate in the Phosphorylation Kinetics of Sodium and Potassium Ion Transport Adenosine Triphosphatase. *Journal of Biological Chemistry* 1972, 247:6530-6540.
3. Albers RW: Biochemical Aspects of Active Transport. *Annual Review of Biochemistry* 1967, 36:727-756.
4. Toyoshima C, Nakasako M, Nomura H, Ogawa H: Crystal structure of the calcium pump of sarcoplasmic reticulum at 2.6 A resolution. *Nature* 2000, 405:647-655.
5. Danko S, Yamasaki K, Daiho T, Suzuki H, Toyoshima C: Organization of cytoplasmic domains of sarcoplasmic reticulum Ca(2+)-ATPase in E(1)P and E(1)ATP states: a limited proteolysis study. *FEBS Lett* 2001, 505:129-135.
6. Toyoshima C, Inesi G: Structural basis of ion pumping by Ca2+-ATPase of the sarcoplasmic reticulum. *Annu Rev Biochem* 2004, 73:269-292.
7. Palmgren MG, Nissen P: P-type ATPases. *Annu Rev Biophys* 2011, 40:243-266.
8. Toyoshima C, Mizutani T: Crystal structure of the calcium pump with a bound ATP analogue. *Nature* 2004, 430:529-535.
9. Toyoshima C: How Ca2+-ATPase pumps ions across the sarcoplasmic reticulum membrane. *Biochim Biophys Acta* 2009, 1793:941-946.
10. Devaux PF: Static and dynamic lipid asymmetry in cell membranes. *Biochemistry* 1991, 30:1163-1173.
11. Takatsu H, Tanaka G, Segawa K, Suzuki J, Nagata S, Nakayama K, Shin HW: Phospholipid Flippase Activities and Substrate Specificities of Human Type IV P-type ATPases Localized to the Plasma Membrane. *J Biol Chem* 2014, 289:33543-33556.
12. Kobayashi T, Menon AK: Transbilayer lipid asymmetry. *Curr Biol* 2018, 28:R386-R391.
13. Shin HW, Takatsu H: Substrates of P4-ATPases: beyond aminophospholipids (phosphatidylserine and phosphatidylethanolamine). *FASEB J* 2019, 33:3087-3096.
14. Roland BP, Naito T, Best JT, Arnaiz-Yepez C, Takatsu H, Yu RJ, Shin HW, Graham TR: Yeast and human P4-ATPases transport glycosphingolipids using conserved structural motifs. *J Biol Chem* 2019, 294:1794-1806.
15. Wang J, Molday LL, Hii T, Coleman JA, Wen T, Andersen JP, Molday RS: Proteomic Analysis and Functional Characterization of P4-ATPase Phospholipid Flippases from Murine Tissues. *Sci Rep* 2018, 8:10795.
16. Naito T, Takatsu H, Miyano R, Takada N, Nakayama K, Shin HW: Phospholipid Flippase

ATP10A Translocates Phosphatidylcholine and Is Involved in Plasma Membrane Dynamics. *J Biol Chem* 2015, 290:15004-15017.

17. Lee S, Uchida Y, Wang J, Matsudaira T, Nakagawa T, Kishimoto T, Mukai K, Inaba T, Kobayashi T, Molday RS, et al.: Transport through recycling endosomes requires EHD1 recruitment by a phosphatidylserine translocase. *EMBO J* 2015, 34:669-688.
18. Coleman JA, Kwok MCM, Molday RS: Localization, Purification, and Functional Reconstitution of the P4-ATPase Atp8a2, a Phosphatidylserine Flippase in Photoreceptor Disc Membranes. *Journal of Biological Chemistry* 2009, 284:32670-32679.
19. Bull LN, van Eijk MJ, Pawlikowska L, DeYoung JA, Juijn JA, Liao M, Klomp LW, Lomri N, Berger R, Scharschmidt BF, et al.: A gene encoding a P-type ATPase mutated in two forms of hereditary cholestasis. *Nat Genet* 1998, 18:219-224.
20. Folmer DE, Elferink RPJO, Paulusma CC: P4 ATPases - Lipid flippases and their role in disease. *Biochimica et Biophysica Acta (BBA) - Molecular and Cell Biology of Lipids* 2009, 1791:628-635.
21. Onat OE, Gulsuner S, Bilguvar K, Nazli Basak A, Topaloglu H, Tan M, Tan U, Gunel M, Ozcelik T: Missense mutation in the ATPase, aminophospholipid transporter protein ATP8A2 is associated with cerebellar atrophy and quadrupedal locomotion. *Eur J Hum Genet* 2013, 21:281-285.
22. Arashiki N, Takakuwa Y, Mohandas N, Hale J, Yoshida K, Ogura H, Utsugisawa T, Ohga S, Miyano S, Ogawa S, et al.: ATP11C is a major flippase in human erythrocytes and its defect causes congenital hemolytic anemia. *Haematologica* 2016, 101:559-565.
23. Alsahli S, Alrifai MT, Al Tala S, Mutairi FA, Alfadhel M: Further Delineation of the Clinical Phenotype of Cerebellar Ataxia, Mental Retardation, and Disequilibrium Syndrome Type 4. *J Cent Nerv Syst Dis* 2018, 10:1179573518759682.
24. Bublitz M, Morth JP, Nissen P: P-type ATPases at a glance. *J Cell Sci* 2011, 124:2515-2519.
25. Vestergaard AL, Coleman JA, Lemmin T, Mikkelsen SA, Molday LL, Vilsen B, Molday RS, Dal Peraro M, Andersen JP: Critical roles of isoleucine-364 and adjacent residues in a hydrophobic gate control of phospholipid transport by the mammalian P4-ATPase ATP8A2. *Proc Natl Acad Sci U S A* 2014.
26. Timcenko M, Lyons JA, Januliene D, Ulstrup JJ, Dieudonne T, Montigny C, Ash MR, Karlsen JL, Boesen T, Kuhlbrandt W, et al.: Structure and autoregulation of a P4-ATPase lipid flippase. *Nature* 2019, 571:366-370.
27. Hiraizumi M, Yamashita K, Nishizawa T, Nureki O: Cryo-EM structures capture the transport cycle of the P4-ATPase flippase. *Science* 2019.
28. Lopez-Marques RL, Poulsen LR, Hanisch S, Meffert K, Buch-Pedersen MJ, Jakobsen MK,

Pomorski TG, Palmgren MG: Intracellular Targeting Signals and Lipid Specificity Determinants of the ALA/ALIS P4-ATPase Complex Reside in the Catalytic ALA {alpha}-Subunit. *Mol. Biol. Cell* 2010, 21:791-801.

29. Bryde S, Hennrich H, Verhulst PM, Devaux PF, Lenoir G, Holthuis JC: CDC50 Proteins Are Critical Components of the Human Class-1 P4-ATPase Transport Machinery. *J Biol Chem* 2010, 285:40562-40572.
30. van der Velden LM, Wichers CGK, van Breevoort AED, Coleman JA, Molday RS, Berger R, Klomp LWJ, van de Graaf SFJ: Heteromeric Interactions Required for Abundance and Subcellular Localization of Human CDC50 Proteins and Class 1 P4-ATPases. *Journal of Biological Chemistry* 2010, 285:40088-40096.
31. Palmgren M, Osterberg JT, Nintemann SJ, Poulsen LR, Lopez-Marques RL: Evolution and a revised nomenclature of P4 ATPases, a eukaryotic family of lipid flippases. *Biochim Biophys Acta Biomembr* 2019, 1861:1135-1151.
32. Lenoir G, Williamson P, Puts CF, Holthuis JCM: Cdc50p Plays a Vital Role in the ATPase Reaction Cycle of the Putative Aminophospholipid Transporter Drs2p. *Journal of Biological Chemistry* 2009, 284:17956-17967.
33. Theorin L, Faxen K, Sorensen DM, Migotti R, Dittmar G, Schiller J, Daleke DL, Palmgren M, Lopez-Marques RL, Gunther Pomorski T: The lipid head group is the key element for substrate recognition by the P4 ATPase ALA2: a phosphatidylserine flippase. *Biochem J* 2019, 476:783-794.
34. Takatsu H, Baba K, Shima T, Umino H, Kato U, Umeda M, Nakayama K, Shin H-W: ATP9B, a P4-ATPase (a Putative Aminophospholipid Translocase), Localizes to the trans-Golgi Network in a CDC50 Protein-independent Manner. *J. Biol. Chem.* 2011, 286:38159-38167.
35. Zhang Y, Werling U, Edelmann W: SLiCE: a novel bacterial cell extract-based DNA cloning method. *Nucleic Acids Res* 2012, 40:e55.
36. Kelley LA, Mezulis S, Yates CM, Wass MN, Sternberg MJ: The Phyre2 web portal for protein modeling, prediction and analysis. *Nat Protoc* 2015, 10:845-858.
37. Andersen JP, Vestergaard AL, Mikkelsen SA, Mogensen LS, Chalat M, Molday RS: P4-ATPases as Phospholipid Flippases-Structure, Function, and Enigmas. *Front Physiol* 2016, 7:275.
38. Axelsen KB, Palmgren MG: Evolution of Substrate Specificities in the P-Type ATPase Superfamily. *J. Mol. Evol.* 1998, 46:84-101.
39. Anthonisen AN, Clausen JD, Andersen JP: Mutational analysis of the conserved TGES loop of sarcoplasmic reticulum Ca2+-ATPase. *J Biol Chem* 2006, 281:31572-31582.
40. Wang G, Yamasaki K, Daiho T, Suzuki H: Critical hydrophobic interactions between

phosphorylation and actuator domains of Ca2+-ATPase for hydrolysis of phosphorylated intermediate. *J Biol Chem* 2005, 280:26508-26516.

41. Marchand A, Winther A-ML, Holm PJ, Olesen C, Montigny C, Arnou B, Champeil P, Clausen JD, Vilsen B, Andersen JP, et al.: Crystal Structure of D351A and P312A Mutant Forms of the Mammalian Sarcoplasmic Reticulum Ca2+-ATPase Reveals Key Events in Phosphorylation and Ca2+ Release. *Journal of Biological Chemistry* 2008, 283:14867-14882.
42. Coleman JA, Molday RS: Critical Role of the b-Subunit CDC50A in the Stable Expression, Assembly, Subcellular Localization, and Lipid Transport Activity of the P4-ATPase ATP8A2. *Journal of Biological Chemistry* 2011, 286:17205-17216.
43. Ding J, Wu Z, Crider BP, Ma Y, Li X, Slaughter C, Gong L, Xie X-S: Identification and Functional Expression of Four Isoforms of ATPase II, the Putative Aminophospholipid Translocase. *Journal of Biological Chemistry* 2000, 275:23378-23386.
44. Coleman JA, Vestergaard AL, Molday RS, Vilsen B, Peter Andersen J: Critical role of a transmembrane lysine in aminophospholipid transport by mammalian photoreceptor P4-ATPase ATP8A2. *Proceedings of the National Academy of Sciences* 2012, 109:1449-1454.
45. Segawa K, Kurata S, Nagata S: Human Type IV P-type ATPases That Work as Plasma Membrane Phospholipid Flippases and Their Regulation by Caspase and Calcium. *J Biol Chem* 2016, 291:762-772.
46. Azouaoui H, Montigny C, Ash MR, Fijalkowski F, Jacquot A, Gronberg C, Lopez-Marques RL, Palmgren MG, Garrigos M, le Maire M, et al.: A high-yield co-expression system for the purification of an intact drs2p-cdc50p lipid flippase complex, critically dependent on and stabilized by phosphatidylinositol-4-phosphate. *PLoS One* 2014, 9:e112176.
47. Takatsu H, Takayama M, Naito T, Takada N, Tsumagari K, Ishihama Y, Nakayama K, Shin HW: Phospholipid flippase ATP11C is endocytosed and downregulated following Ca2+-mediated protein kinase C activation. *Nat Commun* 2017, 8:1423.
48. Takayama M, Takatsu H, Hamamoto A, Inoue H, Naito T, Nakayama K, Shin HW: C-terminal cytoplasmic region of ATP11C variant determines its localization at the polarized plasma membrane. *J Cell Sci* 2019.
49. Holemans T, Sorensen DM, van Veen S, Martin S, Hermans D, Kemmer GC, Van den Haute C, Baekelandt V, Gunther Pomorski T, Agostinis P, et al.: A lipid switch unlocks Parkinson's disease-associated ATP13A2. *Proc Natl Acad Sci U S A* 2015, 112:9040-9045.
50. Braiterman L, Nyasae L, Leves F, Hubbard AL: Critical roles for the COOH terminus of the

Cu-ATPase ATP7B in protein stability, trans-Golgi network retention, copper sensing, and retrograde trafficking. *Am J Physiol Gastrointest Liver Physiol* 2011, 301:G69-81.

51. Chalat M, Moleschi K, Molday RS: C-terminus of the P4-ATPase ATP8A2 functions in protein folding and regulation of phospholipid flippase activity. *Mol Biol Cell* 2017, 28:452-462.
52. Azouaoui H, Montigny C, Dieudonne T, Champeil P, Jacquot A, Vazquez-Ibar JL, Le Marechal P, Ulstrup J, Ash MR, Lyons JA, et al.: High phosphatidylinositol 4-phosphate (PI4P)-dependent ATPase activity for the Drs2p-Cdc50p flippase after removal of its N- and C-terminal extensions. *J Biol Chem* 2017, 292:7954-7970.
53. Natarajan P, Liu K, Patil DV, Sciorra VA, Jackson CL, Graham TR: Regulation of a Golgi flippase by phosphoinositides and an ArfGEF. *Nat Cell Biol* 2009, 11:1421-1426.
54. Segawa K, Kurata S, Nagata S: The CDC50A extracellular domain is required for forming a functional complex with and chaperoning phospholipid flippases to the plasma membrane. *J Biol Chem* 2018, 293:2172-2182.

Figure legends

Figure 1 P-type ATPase catalytic cycle.
(**A, B**) Schematic overview of the structural organization of SERCA (P2A-ATPase) and Drs2p (P4-ATPase), respectively. (**C**) model structure of ATP9A (P4-ATPase) generated by Phyre[2] (http://www.sbg.bio.ic.ac.uk/phyre2/html/page.cgi?id=index) based on the partially activated Drs2p (6ROI). N, nucleotide-binding domain (green); P, phosphorylation domain (blue); A, actuator domain (red). TM1-6 are shown in yellow. (**D**) Sequence alignments of the TGES/DGET motif of the A-domain and the DKTGT sequence motif of the P-domain in human P2A- and P4-ATPases. The conserved TGES/DGET motif (magenta) and DKTGT sequence motif (blue) are indicated. Residues (Gly and Glu of the A-domain and Asp of the P-domain) critical for each transition in (**E**) are indicated (*). (**E**) Schematic overview of the P2A- and P4-ATPase catalytic cycle. Residues critical for the E1–E1P, E1P–E2P, and E2P–E2 transitions in SERCA1a (P2A-ATPase) are indicated.

Figure 2 Cellular localization of ATP11 proteins and their mutants.
(**A, C, E, F, I**) HeLa cells transiently co-expressing C-terminally HA-tagged ATP11A, ATP11B, ATP11C, ATP10A, or its mutant as indicated, and N-terminally FLAG-tagged CDC50A were fixed and stained for HA and ATP1A1 (a marker for the plasma membrane), TfnR (transferrin receptor, a marker for early/recycling endosomes), or Lamp-1 (a marker for late endosomes), followed by incubation with Cy3-conjugated anti–rat antibody and Alexa Fluor 488–conjugated anti–rabbit or anti–mouse secondary antibodies. Scale bars, 20 μm. Enlarged images of the boxed regions are shown on the lines (scale bars, 2 μm). (**B, D, G, J**) HeLa cells transiently co-expressing C-terminally HA-tagged ATP11A, ATP11B, ATP11C, or ATP10A protein or its mutant as indicated, and N-terminally FLAG-tagged CDC50A and EGFP-tagged VAPA (a marker for the ER) were fixed and stained for HA, followed by incubation with Cy3-conjugated anti–rat antibody. Scale bars, 20 μm. Enlarged images of the boxed regions are shown on the lines (scale bars, 2 μm). (**H**) HeLa cells expressing ATP11B or its mutant as indicated were classified into three categories of cellular localization of the ATP11B protein; (1) localized to endosomes (E), (2) localized to endosomes and the ER (E + ER), and (3) localized to the ER only (ER). The number of cells of each category was counted and normalized against the total number of counted cells. In each sample, 112–152 cells were counted. Graphs display averages ± S.D. from three independent experiments.

Figure 3 Interaction of P4-ATPases with endogenous CDC50A.
(**A–F**) HeLa cells stably expressing HA-tagged P4-ATPases and their mutants, and parental cells (-) were lysed and immunoprecipitated with anti-HA antibody. Bound materials were subjected to SDS-PAGE and immunoblotting using anti-HA or anti-CDC50A antibody (**A, C, E**). 10% (WT and EQ mutant) and 5% (GL and DN mutants) of the input of the immunoprecipitation reaction was loaded in each lane (**B, D, F**; total lysate). WT, wild type. * indicates highly glycosylated CDC50A. ATP11A (1135 a.a.), ATP11B (1177, a.a.), ATP11C (1132 a.a.), ATP10A (1499 a.a.), ATP9A (1047 a.a.), ATP9B (1136 a.a.).

Figure 4 Cellular localization of ATP9A and ATP9B and their mutants.
(**A, C, D**) HeLa cells transiently expressing C-terminally HA-tagged ATP9A or ATP9B or its mutant as indicated were fixed and stained for HA and Golgin-245 (a marker for the *trans*-Golgi network, TGN), or TfnR (a marker for early/recycling endosomes), followed by incubation with Cy3-conjugated anti–rat antibody and Alexa Fluor 488–conjugated anti–mouse secondary antibodies. (**B, E**) HeLa cells transiently co-expressing C-terminally HA-tagged ATP9A or ATP9B and EGFP-tagged VAPA (a marker for the ER) were fixed and stained for HA, followed by incubation with Cy3-conjugated anti–rat antibody. Scale bars, 20 μm. Enlarged images of the boxed regions are shown on the bottom lines (scale bars, 2 μm). (**F**) HeLa cells expressing ATP9B or its mutant as indicated were classified into three categories of cellular localization of the ATP9B protein; (1) localized to the Golgi (Golgi), (2) localized to the Golgi and the ER (Golgi + ER), and (3) localized to the ER only (ER). The number of cells of each category was counted and normalized against the total number of counted cells. In each sample, 115–151 cells were counted. Graphs display averages ± S.D. from three independent experiments.

Supplementary Figure legends

Supplementary Figure S1 Specificity of anti–CDC50A antibody.
(**A**) HeLa cells transiently expressing N-terminally FLAG-tagged CDC50A or CDC50B were lysed, subjected to SDS-PAGE, and analyzed by immunoblotting with anti–CDC50A, anti–DYKDDDDK, or anti–β-tubulin antibody. The membrane was stained with Ponceau S. (**B**) The cell lysates were immunoprecipitated with anti–DYKDDDDK antibody and analyzed by immunoblotting with anti–CDC50A or anti–DYKDDDDK antibody.

Supplementary Figure S2 Localization of ATP9 proteins in the presence or absence of exogenous CDC50A expression.
HeLa cells were transiently co-transfected with an expression vector for C-terminally HA-tagged ATP9A or ATP9B, or its mutant as indicated and a vector for N-terminally FLAG-tagged CDC50A. After 48 h of transfection, the cells were processed for immunofluorescence microscopy. The cells were stained for HA and FLAG, followed by incubation with Cy3-conjugated anti–rat and Alexa Fluor 488–conjugated anti–mouse antibodies. Insets indicate CDC50A expression. Scale bars, 20 μm.

Supplementary Figure S3 Cellular localization of P4-ATPases and their mutants in stably expressing cells.
HeLa cells stably expressing HA-tagged P4-ATPases and their mutants were fixed and stained for HA and Golgin-245, ATP1A1, or TfnR followed by incubation with Cy3-conjugated anti–rat antibody and Alexa Fluor 488–conjugated anti–rabbit or anti–mouse secondary antibodies. Scale bars, 20 μm.

Supplementary Table Oligonucleotides used for mutagenesis in this study.

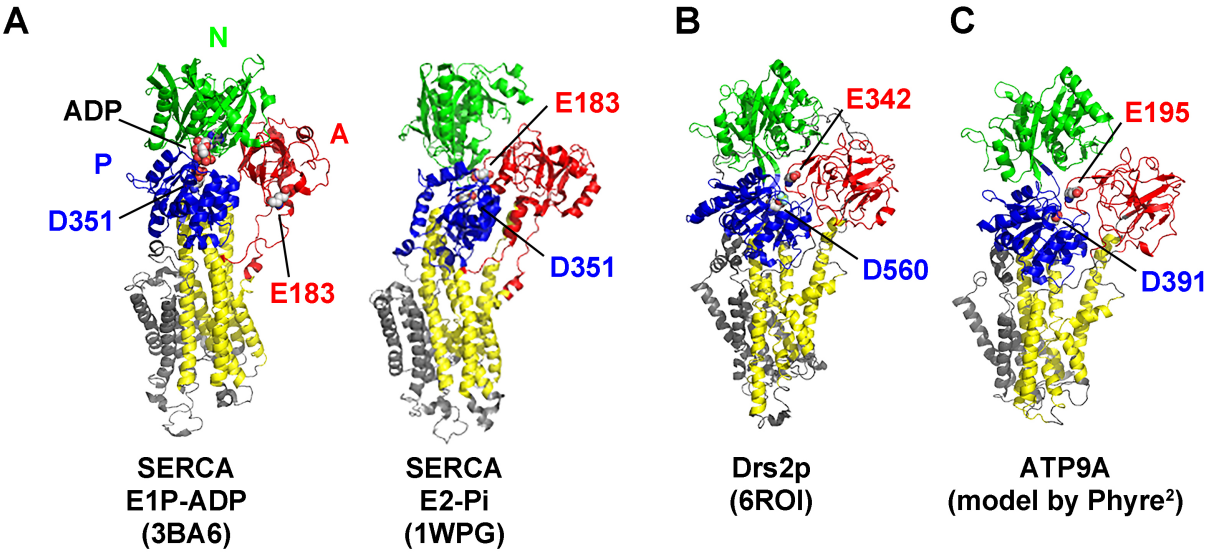

D

	A domain	P domain
	**	*
*hs*Serca	SILTGESVSVIKH	VICSDKTGTLTTNQM
*hs*Na⁺/K⁺-pump	SSLTGESEPQTRS	TICSDKTGTLTQNRM
*sc*Drs2p	ANLDGETNLKIKQ	YIFSDKTGTLTRNIM
*hs*ATP8A1	SNLDGETNLKIRQ	YIFSDKTGTLTCNVM
*hs*ATP8B1	AELDGETNLKFKM	YIFSDKTGTLTQNIM
*hs*ATP9A	DQLDGETDWKLRL	YLLTDKTGTLTQNEM
*hs*ATP9B	DQLDGETDWKLKV	YLLTDKTGTLTQNEM
*hs*ATP10A	ANLDGETNLKRRQ	YIFSDKTGTLTENKM
*hs*ATP10B	ASLDGETNLKQRC	YIFSDKTGTLTENKM
*hs*ATP10D	SGLDGESNLKQRQ	YLFSDKTGTLTENKM
*hs*ATP11A	ASLDGESSHKTHY	YIFTDKTGTLTENNM
*hs*ATP11B	ASLDGETNLKTHV	YVFTDKTGTLTENEM
*hs*ATP11C	ASLDGESNCKTHY	YVFTDKTGTLTENSM

E

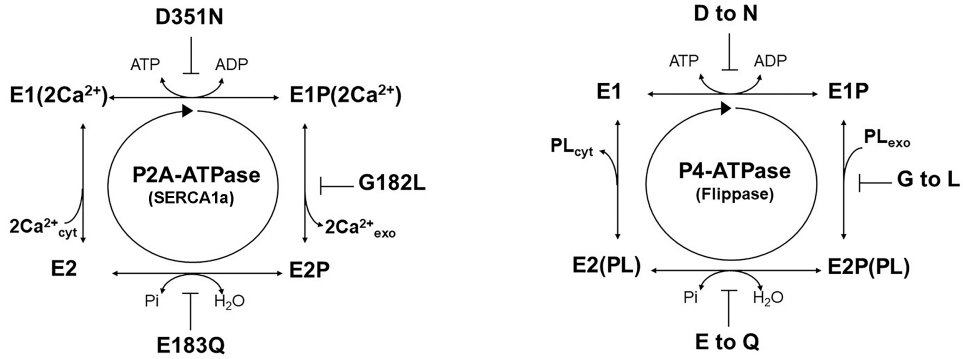

Figure 1 Tone et al.

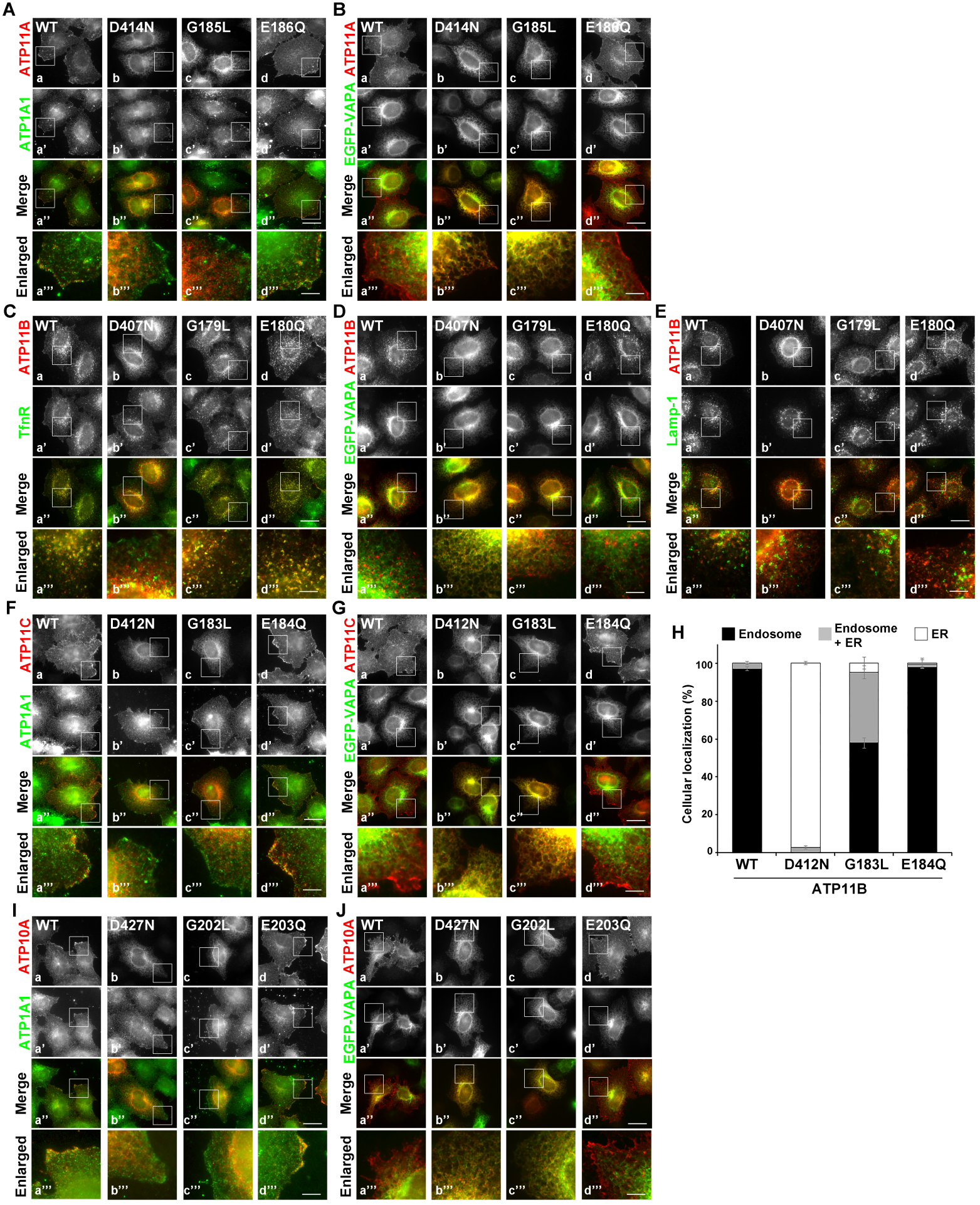

Tone et al. Figure 2

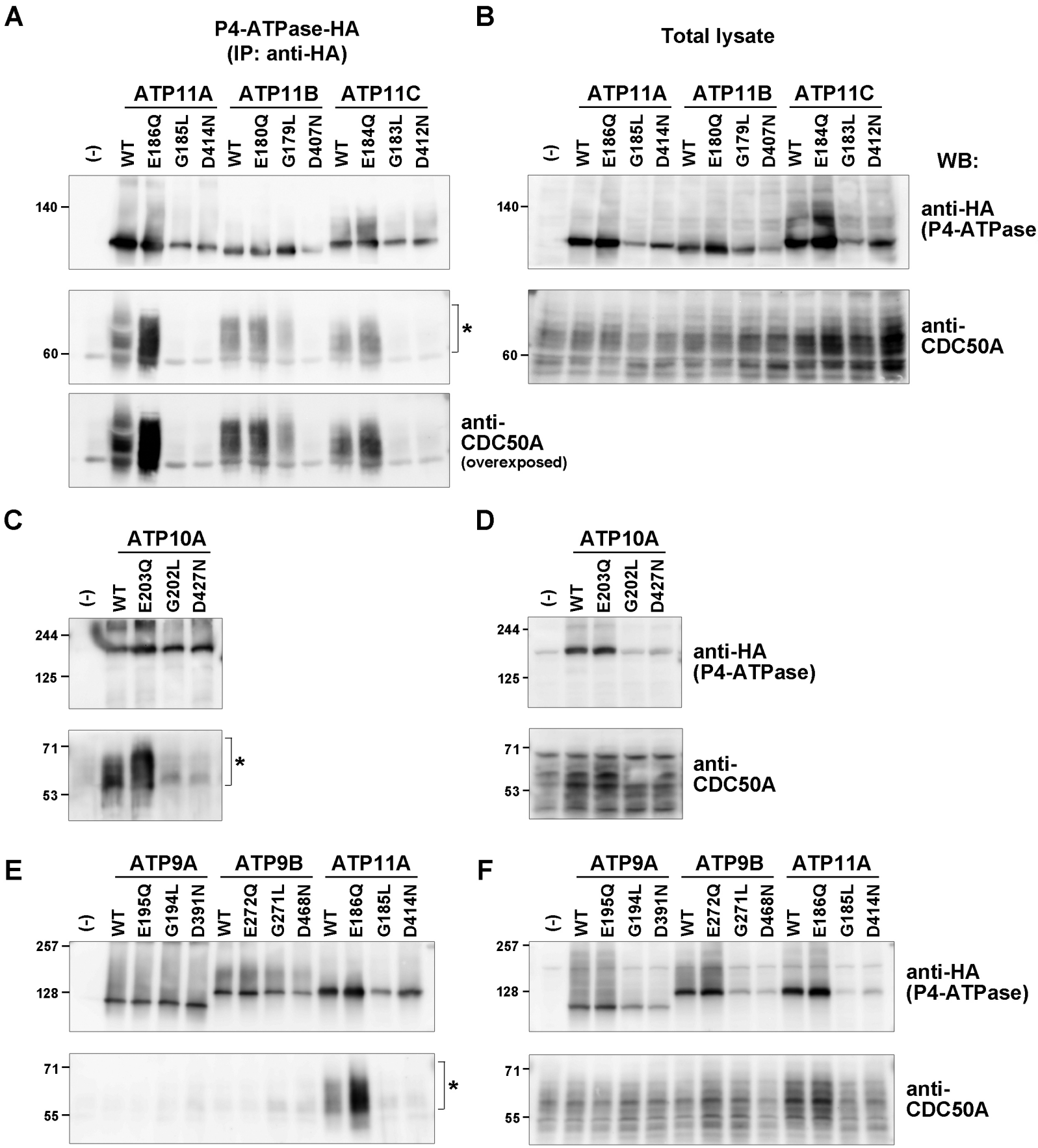

Figure 3 Tone et al.

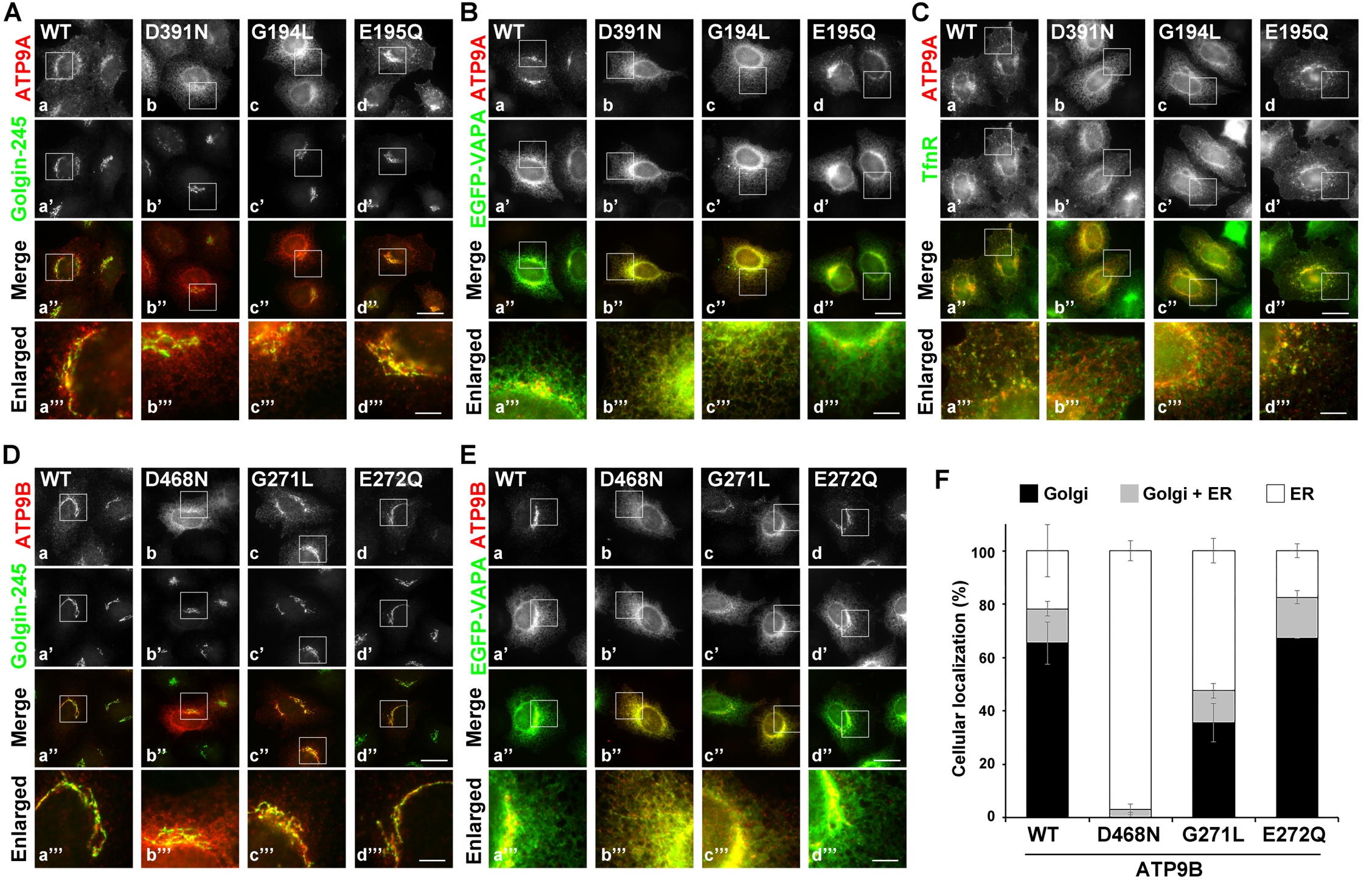

Figure 4 Tone et al.

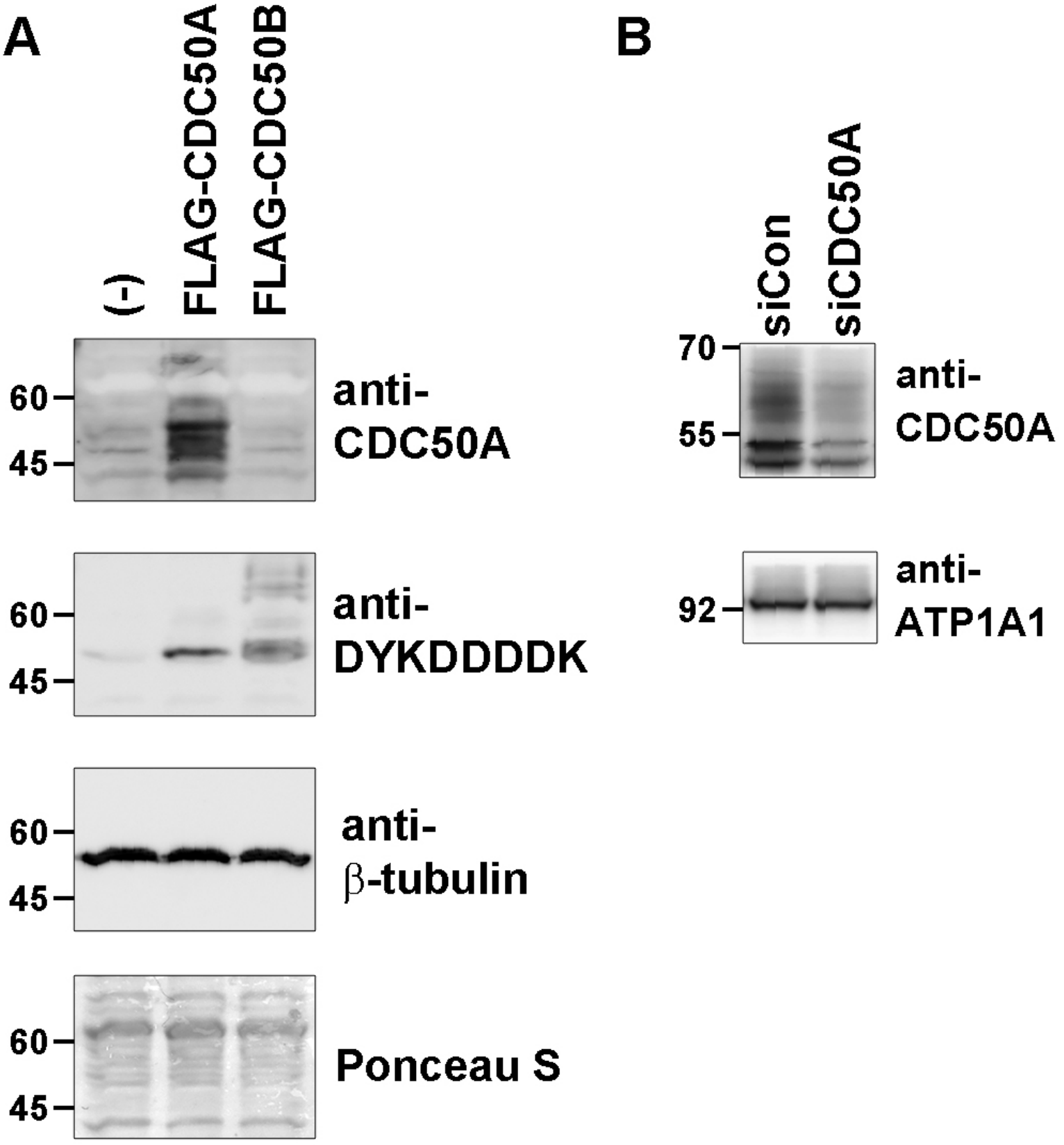

Supplementary Figure S1 Tone et al.

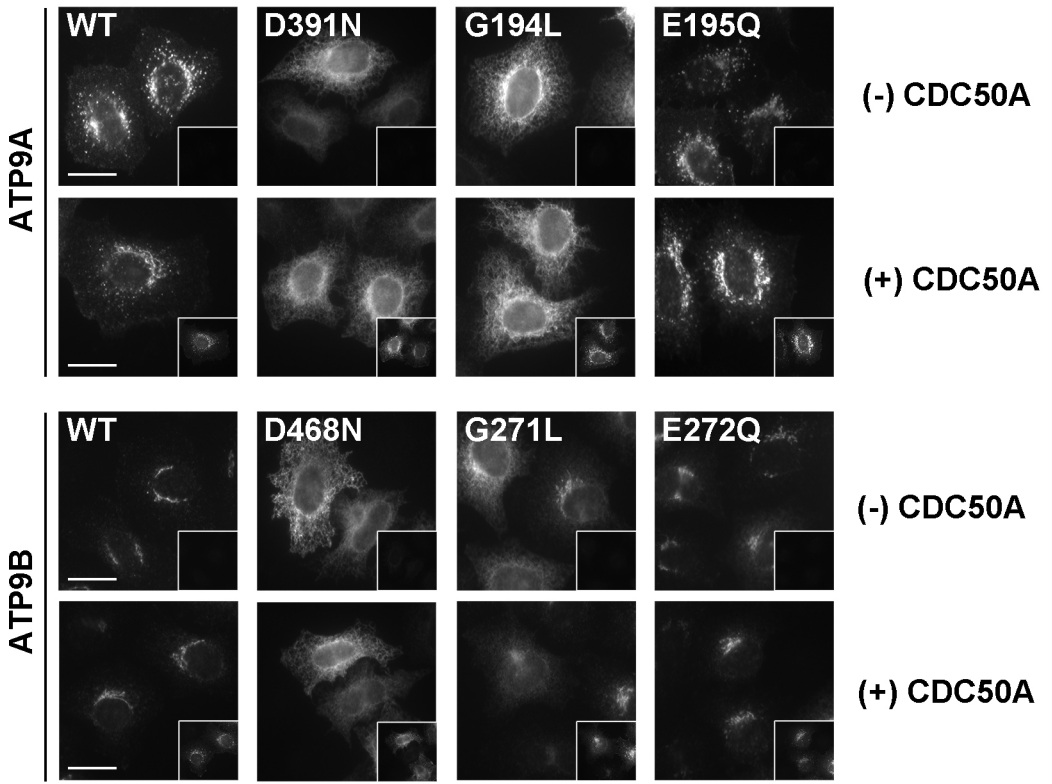

Supplementary Figure S2 Tone et al.

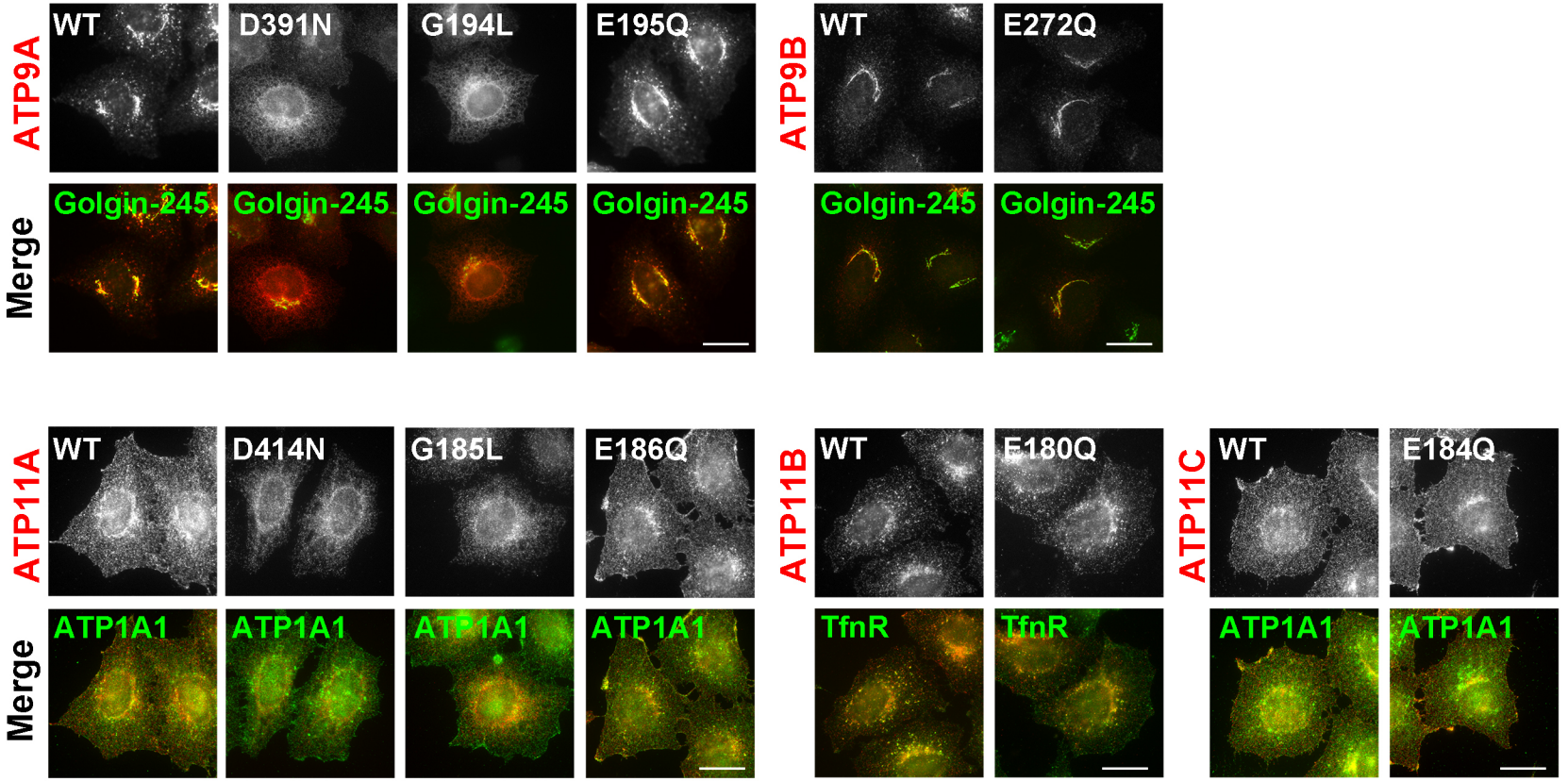

Supplementary Figure S3 Tone et al.

Supplementary Table Tone et al.

Mutation	Primer	Sequences (5'---- 3')	
hATP9A (G194L)	sense	agctggatctggagacggactggaagctg	This study
	antisense	tccgtctccagatccagctgatccgtccgc	This study
hATP9A (E195Q)	sense	ggatcagctggatgggcagacggactggaagctg	This study
	antisense	cagcttccagtccgtctgcccatccagctgatcc	This study
hATP9A (D391N)	sense	ttactcacaaacaagacaggcactcttacc	This study
	antisense	ctgtcttgtttgtgagtaagtacgaaatcctg	This study
hATP9B (G271L)	sense	aactagatctcgaaactgactggaagctgaag	This study
	antisense	tcagtttcgagatctagttgatcagttcgaata	This study
hATP9B (E272Q)	sense	cgaactgatcaactagatggtcaaactgactggaagctgaaggtg	This study
	antisense	caccttcagcttccagtcagtttgaccatctagttgatcagttcg	This study
hATP9B (D468N)	sense	gcctggtgtatttattgacaaacaaaacaggaaccctcaccc	This study
	antisense	gggtgagggttcctgttttgtttgtcaataaatacaccaggc	This study
hATP10A (G202L)	sense	acctggatctagagaccaacctgaagcgg	This study
	antisense	ttggtctctagatccaggttggcggtctcg	This study
hATP10A (E203Q)	sense	gagaccgccaacctggatggacagaccaacctgaagcggcgg	[16]
	antisense	ccgccgcttcaggttggtctgtccatccaggttggcggtctc	[16]
hATP10A (D427N)	sense	attttctcaaataaaactggcactttgacagag	This study
	antisense	cagttttatttgagaaaatgtactgtatctgtcc	This study
hATP11A (G185L)	sense	gcttggatctagaatccagccataaaacgc	This study
	antisense	ctggattctagatccaagctggcggtggtg	This study
hATP11A (E186Q)	sense	caccgccagcttggatggacaatccagccataaaacgcattac	[11]
	antisense	gtaatgcgttttatggctggattgtccatccaagctggcggtg	[11]
hATP11A (D414N)	sense	gacaggtggagtacatcttcacaaacaagaccggcaccctcacg	[11]
	antisense	cgtgagggtgccggtcttgtttgtgaagatgtactccacctgtc	[11]
hATP11B (G179L)	sense	gtttggacctcgaaactaacctgaagacacatg	This study
	antisense	ttagtttcgaggtccaaactagcagttgtaac	This study
hATP11B (E180Q)	sense	ctgctagtttggacggacaaactaacctgaagacac	This study
	antisense	gtgtcttcaggttagtttgtccgtccaaactagcag	This study
hATP11B (D407N)	sense	gtgtttacaaataaaactggtacactgacag	This study
	antisense	cagttttatttgtaaacacgtactctacctg	This study

hATP11C (G183L)	sense	gtcttgatctggaatccaattgcaagacac	This study
	antisense	ttggattccagatcaagactggctgtagtgac	This study
hATP11C (E184Q)	sense	cactacagccagtcttgatgggcaatccaattgcaagacacattatgc	[11]
	antisense	gcataatgtgtcttgcaattggattgcccatcaagactggctgtagtg	[11]
hATP11C (D412N)	sense	ggtcaggtggattatgtatttacaaataagactggaacactcactg	[11]
	antisense	cagtgagtgttccagtcttatttgtaaatacataatccacctgacc	[11]